NASA Technical Paper 2599

September 1986

Motion and Interaction of Decaying Trailing Vortices in Spanwise Shear Wind

Chen-Huei Liu
and Lu Ting

NASA

NASA Technical Paper 2599

1986

Motion and Interaction of Decaying Trailing Vortices in Spanwise Shear Wind

Chen-Huei Liu
Langley Research Center
Hampton, Virginia

Lu Ting
New York University
New York, New York

National Aeronautics
and Space Administration

Scientific and Technical Information Branch

SYMBOLS

C	adjustable constant
D	computational domain
H	integration domain size used for averaging (eq. (29b))
$\hat{i},\hat{j}$	unit vectors in x- and y-directions, respectively
L	reference height of background shear flow (reference length scale)
L_1,L_2	size of computational domain in streamwise and vertical directions, respectively (fig. 2)
$O(\ )$	of the order of
R_L	Reynolds number of background flow, $U_\infty L/\nu$
r_k	distance from kth vortical center
t	time
t_k	initial age of vortical spot, $\delta_k^2(0)/4\nu$
$U_0(y)$	upstream (spanwise) flow
U_∞	reference velocity scale, $U_0(\infty)$
u,v	velocity components in x- and y-directions, respectively
$\vec{V}$	velocity vector
$(\bar{v}_\theta)_k$	circumferential velocity around kth vortical spot
X_y,Y_k	kth vortical center
$\dot{X}_k(t),\dot{Y}_k(t)$	velocity of kth vortical spot
$X_R - X_L$	horizontal spread of right and left vortex of pair
x,y,z	spanwise, vertical, and flight directions, respectively
Y_R	vertical position of right vortex of pair
Γ	strength of vortical spot
δ	effective core size of vortical spot (small length scale)
ε	small parameter, $\delta/L \ll 1$
$\zeta(x,y,t)$	vorticity distribution
ν	kinematic viscosity

ρ distance from origin of coordinates, $(x^2 + y^2)^{1/2}$

$\psi(x,y,t)$ stream function

$\omega(x,y,t)$ background vorticity distribution

Δt time step

$\Delta x, \Delta y, \Delta L$ grid sizes

∇^2 Laplacian operator

Subscripts:

k kth vortical spot

L left

min minimum

R right

$\bar{x}$ $= \partial/\partial\bar{x}$

$\bar{y}$ $= \partial/\partial\bar{y}$

0 reference initial quantity at $t = 0$

Notation:

$(\bar{})$ bar quantity denotes terms of small parameter

$(\tilde{})$ tilde quantity denotes variation of background flow quantity

$( )'$ derivative of quantity

$< >$ average of flow quantity (eq. (29b))

SUMMARY

The drift of trailing vortices in a crosswind near the ground is simulated by an unsteady, two-dimensional, rotational flow field with a concentration of large vorticity in "vortical spots" (having a finite but small effective size and finite total strength). The problem is analyzed by a combination of the method of matched asymptotic analyses for the decay of the vortical spots and the Euler solution for the unsteady rotational flow. Using the method of averaging, a special numerical method is developed in which the grid size and time step depend only on the length and velocity scales of the background flow and are independent of the effective core size of a vortical spot. The core size can be much smaller than the grid size, whereas the peak velocity in the core is inversely proportional to the spot size. Numerical results are presented to demonstrate the strong interaction between the trajectories of the vortical spots and the change of the vorticity distribution in the background flow field.

1 INTRODUCTION

It has been well-recognized that there is a potential hazard whenever a small aircraft encounters the vortex wake of a larger aircraft, particularly during the takeoff and landing phase of the aircraft. An understanding of the motion and structure of the vortex wake, including the ground effect and its minimization, is important for flight safety and also for efficient use of the airport (refs. 1 and 2).

The variation of the vortex wake strength along the trailing edge of the lifting wing depends on the characteristics of the wing. Complete prediction of the flow field including the near wake is very difficult because of the disparate length scales associated with the generation, interaction, and eventual decay of the vortices. The problem of a steady far-wake vortex can be simplified by reducing the problem to an equivalent unsteady two-dimensional problem in a plane normal to the flight direction (ref. 3). This assumption ignores the streamwise curvature of the trailing vortex filaments, their initiation at the trailing edge, and the variation of the velocity parallel to the downstream direction (z). Mathematically, it is assumed that $\partial/\partial z \ll \partial/\partial x$ and $\partial/\partial z \ll \partial/\partial y$, where x and y are the spanwise and vertical directions, respectively. In the xy-plane at a station z, the trailing vortices are represented by "vortical spots" (having a small effective size inside which there is a strong vorticity distribution with finite total strength).

This simulation is employed to study the drift and decay of far-field trailing vortices (vortical spots) in a crosswind (a spanwise shear flow) near the ground. Note that the Reynolds number R_L of the background flow can be much larger than 1, i.e.,

$$R_L = \frac{U_\infty L}{\nu} \gg 1 \qquad (1)$$

where U_∞, L, and ν are the reference velocity, the height of the background shear flow, and the kinematic viscosity, respectively. Since the size of a vortical spot is much smaller than L and its total strength Γ is finite, i.e., of the order of $U_\infty L$, the vorticity and the velocity gradients in a spot can be very large. Thus, the diffusion in the core of a vortical spot is important; but away from it, the viscous term is of the order of $1/R_L$ and, hence, is negligible.

It is very inefficient to study the flow field of vortical spots submerged in a rotational flow by numerical solution of the Navier-Stokes equations for the entire flow field since the viscous terms are important only in small spots of high vorticity concentration and the grid size would have to be smaller than the size of the spots. A multiple-scale analysis is introduced in order to isolate the viscous decay of vorticity in the spots as a solution of the "small" scale variables, whereas the flow field in the "normal" scale obeys the Euler equations. The decay of the vortical core in each spot can then be described by a matched asymptotic solution (ref. 4), and the motion of the vortical spots is coupled with the variation of the vorticity distribution in the background nonuniform shear flow, requiring a numerical solution of the unsteady Euler equations.

It is noted here that if the background flow is a constant shear flow (constant vorticity) or a potential flow (zero vorticity), the movements of a vortical spot cannot induce any variation in the background vorticity distribution and will not change the background flow. Therefore, the flow field can be represented as the superposition of the steady background flow and that induced by the moving vortical spots defined by the asymptotic analysis.

Section 2 presents a description of the governing equations and the scaling laws for the mathematical simulation of the interaction of the vortex wake with a cross-wind. The asymptotic solutions for the decaying vortical spots are described. In this simulation, the background flow (without the vortical spots) fulfills the non-slip condition along the ground. The unsteady boundary layer along the wall (or ground) induced by a vortical spot has not been accounted for in the Euler solution. Therefore, the distance from a vortical spot to the wall should remain much larger than the thickness of the boundary layer induced by the vortical spots.

In section 3, a special numerical method that implements the concept of a two-length scale analysis is described for the solution of the Euler equation. Consequently, the step size and the time step will be independent of the effective size of the vortical spots (which can be much smaller). Note that the peak velocity in the core, being inversely proportional to the core size, can be much larger than U_∞.

In section 4, numerical results are presented to demonstrate the interactions between the vortical spot and the background nonuniform shear flow. The distinct features of the trajectories of vortical spots with varying strengths and different initial positions are illustrated.

2 MATHEMATICAL FORMULATION

2.1 The Physical Problem (Upstream and Initial Conditions)

The physical simulation for the motion and decay of strong two-dimensional vortical spots interacting with a background rotational flow is illustrated in figure 1. An upstream (spanwise) flow $U_0(y)$ is specified, i.e.,

$$\vec{V}(x,y,0) = U_0(y)\,\hat{i} = O(1) \tag{2a}$$

as $x \to -\infty$ for $y \geq 0$ with $U_0(0) = 0$. The ground is represented by $y = 0$. The background rotational flow has the reference length scale L, which is equal to the effective height of the shear flow, and the reference velocity scale U_∞, which is $U_0(\infty)$. Both scales, L and U_∞, have been set equal to 1. It is assumed that $U_0(y) \to 1$ exponentially in y as $y \to \infty$, e.g.,

$$U_0(y) = 1 - e^{-y} \tag{2b}$$

The corresponding initial background vorticity distribution is then

$$\omega(x,y,0) = -U_0'(y) = O(1) \tag{2c}$$

To simulate the trailing vortices, a highly concentrated vortical spot, say the kth spot centered at $(X_k(0), Y_k(0))$, is defined by the following characteristics: an initially small effective core size ($\delta_k(0) \ll 1$) and a strong vorticity distribution ($\zeta_k = O(\delta_k^{-2}) \gg 1$) so that the total strength is finite ($\Gamma_k = O(1) = O(U_\infty L)$).

Because of these characteristics of vortical spots, it is assumed that the initial vorticity distribution $\zeta(x,y,0)$ can be split into two parts and that

$$\zeta(x,y,0) = \omega(x,y,0) + \varepsilon^{-2}\,\bar{\zeta}(\bar{x},\bar{y},0) \tag{3}$$

where

$$\varepsilon = \delta/L \ll 1 \tag{4}$$

and δ is the typical core size. The second term $\varepsilon^{-2}\,\bar{\zeta}(\bar{x},\bar{y},0)$ in equation (3) with $\bar{\zeta} = O(1)$ represents concentrated vorticity distributions near the vortical spot. This vorticity distribution is of compact support or decays exponentially in $\bar{r}_k$, where $\bar{r}_k$ is the distance from the kth center in terms of the small length scale δ. One can then write $\bar{\zeta}$ as a function of the stretched variables $\bar{x}$ and $\bar{y}$ with

$$\bar{x}_k = \frac{x - X_k}{\varepsilon} \qquad \bar{y}_k = \frac{y - Y_k}{\varepsilon} \tag{5}$$

for each k. For simplicity, the case considered here is that of vortical spots having similar core structures (such as a Lamb vortex (ref. 5)), i.e.,

$$\varepsilon^{-2}\bar{\zeta} = \sum_{k=1}^{N} \varepsilon^{-2}\,\bar{\zeta}_k(\bar{x},\bar{y},0) = \sum_{k=1}^{N} \frac{\Gamma_k}{\pi\,\delta_k^2(0)}\, e^{-\left\{\bar{r}_k[\varepsilon/\delta_k(0)]\right\}^2} \tag{6}$$

where

$$\bar{r}_k = \left\{[x - X_k(0)]^2 + [y - Y_k(0)]^2\right\}^{1/2}\Big/\varepsilon$$

From the initial vorticity distribution, it is noted that (1) the initial vortex positions $(X_k(0), Y_k(0))$ are assigned, (2) $\bar{\zeta}_k$ decays exponentially in $\bar{r}_k$, and (3) the strength Γ_k is assumed to be of the order $U_\infty L$, i.e.,

$$\Gamma_k = \int_{-\infty}^{\infty}\!\!\int \varepsilon^{-2}\bar{\zeta}_k\, dx\, dy = \int_{-\infty}^{\infty}\!\!\int \bar{\zeta}_k\, d\bar{x}_k\, d\bar{y}_k = O(U_\infty L) \tag{7}$$

This analysis can take care of nonsimilar initial profiles, i.e., not of the type specified by equation (6), as long as $\bar{\zeta}_k$ decays exponentially in $\bar{r}_k$ and fulfills equation (7).

2.2 Governing Equations

For an unsteady viscous flow field, the vorticity distribution $\zeta(x,y,t)$ and the stream function $\psi(x,y,t)$ are governed by the two equations

$$\frac{\partial\zeta}{\partial t} + \frac{\partial}{\partial x}(u\zeta) + \frac{\partial}{\partial y}(v\zeta) = \nu\nabla^2\zeta \tag{8}$$

and

$$\nabla^2\psi = -\zeta \tag{9}$$

where ∇^2 is the Laplacian operator. The vorticity is defined by

$$\zeta = \frac{\partial v}{\partial x} - \frac{\partial u}{\partial y} \tag{10}$$

and the velocity components are related to the stream function by

$$u = \frac{\partial \psi}{\partial y} \qquad v = -\frac{\partial \psi}{\partial x} \tag{11}$$

The boundary conditions along the ground plane are

$$u(x,0,t) = 0 \tag{12}$$

and

$$v(x,0,t) = 0 \tag{13}$$

In general, to construct the Navier-Stokes solution of equations (8) and (9), one has to use grid sizes Δx and $\Delta y << \delta$ and, hence, a very small Δt. This process is very inefficient since the viscous term $\nu\nabla^2\zeta$ is important only in the neighborhood of a vortical spot (of the order δ); and away from it, the viscous term is not important.

In section 3, a special method is described that takes into account the special features of the vorticity distribution. It should be recognized that the flow field also has a small length scale δ, i.e., εL. The small parameter ε is of the order of $1/R_L^{1/2}$; i.e.,

$$\varepsilon = \frac{\delta}{L} = O\left(\frac{1}{R_L^{1/2}}\right) = O\left(\frac{\nu}{\Gamma_k^{1/2}}\right) \tag{14}$$

so that the viscous terms remain important in the small scale, i.e., in the neighborhood of a vortical spot. On the other hand, in the normal scale, the flow field obeys the Euler equations.

3 METHOD OF SOLUTION

In subsection 3.1, the problem is set up in two length scales, the normal scale L and the small scale $\delta = \varepsilon L$. Analytical solutions describing the "small" scale flow field (i.e., the viscous decay of the strong vorticity in each vortical spot) will be identified as that of the similarity solution from the asymptotic analysis (refs. 6 and 7). The velocity $(\dot{X}_k(t), \dot{Y}_k(t))$ of the kth vortical spot is coupled with the inviscid solutions describing the "normal" scale flow field (i.e., the background flow). In subsection 3.2, the details will be described about the method for constructing the numerical solution of the variation of vorticity in the background shear flow. A particular feature of the numerical method is that the grid size $\Delta x = \Delta y = \Delta L$ can be selected independent of the core size δ_k. The time step

depends only on the grid size and on the length and velocity scales of the background flow, i.e.,

$$\Delta t = f(\Delta L, U_\infty) \tag{15}$$

3.1 The Two-Length-Scale Problem

The special form of the initial data suggests the following decomposition of vorticity:

$$\zeta(x,y,t) = \omega_0(y) + \tilde{\zeta}(x,y,t,\varepsilon) + \varepsilon^{-2}\,\bar{\zeta}(\bar{x},\bar{y},t,\varepsilon) \tag{16}$$

Here, x and y denote the regular spatial variables and $\bar{x} = x/\varepsilon$ and $\bar{y} = y/\varepsilon$ denote the stretched variables. The first term $\omega_0(y)$ in equation (16) is the initial background vorticity. The second term $\tilde{\zeta}(x,y,t,\varepsilon)$ is the variation of background vorticity induced by the vortical spots. The last term is composed of the large vorticity $O(\varepsilon^{-2})$ near the vortical spot, i.e.,

$$\varepsilon^{-2}\bar{\zeta} = \varepsilon^{-2} \sum_k \bar{\zeta}_k(\bar{x}_k,\bar{y}_k,t,\varepsilon) \tag{17}$$

Here, $\bar{\zeta}_k$ decays exponentially in

$$\bar{r}_k = \left\{[x - X_k(t)]^2 + [y - Y_k(t)]^2\right\}^{1/2}\Big/\varepsilon$$

Similarly, the stream function can be written as

$$\psi(x,y,t) = \psi_0(y) + \tilde{\psi}(x,y,t,\varepsilon) + \bar{\psi}(\bar{x},\bar{y},t,\varepsilon) \tag{18}$$

The velocity components can also be decomposed into

$$\vec{V} = \left[U_0(y) + \tilde{u} + \varepsilon^{-1}\bar{u}\right]\hat{i} + (\tilde{v} + \varepsilon^{-1}\bar{v})\hat{j} \tag{19}$$

and can be related to $\tilde{\psi}$ and $\bar{\psi}$ by

$$\tilde{u} = \frac{\partial \tilde{\psi}}{\partial y} \qquad \tilde{v} = -\frac{\partial \tilde{\psi}}{\partial x} \tag{20}$$

and

$$\bar{u} = \frac{\partial \bar{\psi}}{\partial \bar{y}} \qquad \bar{v} = -\frac{\partial \bar{\psi}}{\partial \bar{x}} \tag{21}$$

The velocity fields are then described by the stream functions, which in turn are related to the vorticity functions by

$$\psi_0(y) = \int_0^y U_0(y')\, dy' \tag{22}$$

$$\bar{\nabla}^2 \bar{\psi} = -\bar{\zeta} \tag{23}$$

and

$$\nabla^2 \tilde{\psi} = -\tilde{\zeta} \tag{24}$$

The boundary condition on the ground ($y = 0$) for the velocity field is $v(x,0,t) = 0$. The nonslip condition shall be taken care of by the addition of a thin boundary layer induced by the vortical spots. By following the method of multiple scales, the decomposition equations (eqs. (16) to (19)) are substituted into equations (8) and (9) and the variables x, y, $\bar{x}$, and $\bar{y}$ are treated as independent. By collecting terms of equal powers of ε, one obtains the leading solution involving $(\bar{x}, \bar{y})$, i.e., the analytical solution near each vortical spot. For the kth spot centered at $(X_k(t), Y_k(t))$, the solution is (refs. 4 and 6)

$$\varepsilon^{-2}\bar{\zeta}_k \approx \varepsilon^{-2}\bar{\zeta}(0) = \frac{\Gamma_k}{\pi\, \delta_k^2(t)}\, e^{-\varepsilon^2 \bar{r}_k^2/\delta_k^2(t)} \tag{25}$$

where

$$\delta_k(t) = \delta_k(0)\, [(t + t_k)/t_k]^{1/2}$$

is the effective core size and $t_k = \delta_k^2(0)/4\nu$ is the initial age of the vortical spot. Here the superscript (0) denotes "the leading term of." The use of the similarity solution is explained in reference 4. Note that the solution given by equation (25) has only a "short range" effect because of exponential decay. On the other hand, the corresponding velocity is given by

$$\varepsilon^{-1}\left(\bar{u}_k\hat{i} + \bar{v}_k\hat{j}\right) = \left[\varepsilon^{-1}(\bar{v}_\theta)_k\left(\bar{x}_k\hat{j} - \bar{y}_k\hat{i}\right)\right]\Big/\bar{r}_k \tag{26a}$$

with

$$\varepsilon^{-1}(\bar{v}_\theta)_k = \frac{\Gamma_k}{2\pi\varepsilon\bar{r}_k}\left(1 - e^{-\varepsilon^2\bar{r}_k^2/\delta_k^2}\right) \tag{26b}$$

and

$$\bar{x}_k = \bar{x} - (X_k/\varepsilon) \qquad \bar{y}_k = \bar{y} - (Y_k/\varepsilon)$$

Here, $\varepsilon^{-1}(\bar{v}_\theta)_k$ denotes the circumferential velocity around the kth vortical spot and does not decay exponentially but has a "long range" effect, i.e.,

$$(\bar{v}_\theta)_k \approx \frac{\Gamma_k}{2\pi\bar{r}_k} \tag{27}$$

This effect provides the coupling with the background flow. From an asymptotic analysis (refs. 4 and 6), the velocity of the center of the kth spot $(\dot{X}_k, \dot{Y}_k)$ is established to be equal to the local velocity without the kth vortical spot, i.e., at (X_k, Y_k),

$$\dot{X}_k\hat{i} + \dot{Y}_k\hat{j} = U_0(Y_k)\,\hat{i} + \tilde{u}(X_k,Y_k)\,\hat{i} + \tilde{v}(X_k,Y_k)\,\hat{j} + \sum_{j\neq k}\varepsilon^{-1}\left(\bar{u}_j\hat{i} + \bar{v}_j\hat{j}\right) \tag{28}$$

This result is in agreement with classical inviscid theory. The motion of the vortical spots is, in turn, coupled with the variation of the background vorticity distribution $\tilde{\zeta}$ that is O(1) and is a function of the normal spatial variables. In subsection 3.2, the method for the solution of $\tilde{\zeta}(x,y,t)$ will be described.

3.2 Background Flow Field

To derive the governing equations for the background flow field in the normal length scale, the details of the flow structure need to be filtered out in the small length scale εL. This procedure is accomplished by averaging the basic equations (eqs. (8) and (9)) over an area of, say, a square of side $2H$ where H is much larger than the core size εL but much smaller than L, i.e.,

$$L >> H >> \varepsilon L \tag{29a}$$

In the following equation, $\langle f \rangle$ is used to denote the average of $f(x,y,\bar{x},\bar{y})$, i.e.,

$$\langle f \rangle = \frac{\varepsilon^2}{4H^2} \int_{(y-H)/\varepsilon}^{(y+H)/\varepsilon} \int_{(x-H)/\varepsilon}^{(x+H)/\varepsilon} f(x,y,\bar{x},\bar{y})\, d\bar{x}\, d\bar{y} \tag{29b}$$

With f bounded for all $(\bar{x}, \bar{y})$, the result is

$$\left\langle \frac{\partial f}{\partial \bar{x}} \right\rangle = 0 \qquad \left\langle \frac{\partial f}{\partial \bar{y}} \right\rangle = 0 \tag{30a}$$

For a function $g(x,y)$ having no microstructure, i.e., independent of $\bar{x}$ and $\bar{y}$, the result is

$$\langle g \rangle = g(x,y) \tag{30b}$$

Using equations (29b) and (30), the average of equations (8) and (9) yields the leading equations for the variation of background vorticity $\tilde{\zeta}(x,y,t)$ and the corresponding stream function $\tilde{\psi}(x,y,t)$; i.e.,

$$\frac{\partial \tilde{\zeta}}{\partial t} + \frac{\partial}{\partial x}\{[U_0(y) + \tilde{u}(x,y,t) + \langle \varepsilon^{-1}\bar{u}\rangle]\tilde{\zeta}\} + \frac{\partial}{\partial y}\{[\tilde{v}(x,y,t) + \langle \varepsilon^{-1}\bar{v}\rangle]\tilde{\zeta}\}$$

$$+ [\tilde{v} + \langle \varepsilon^{-1}\bar{v}\rangle]\frac{d\omega_0}{dy} = 0 \tag{31}$$

and

$$\nabla^2\tilde{\psi} = -\tilde{\zeta} \tag{32}$$

The initial and boundary conditions are, respectively,

$$\tilde{\zeta} = 0 \qquad (t = 0) \qquad (33)$$

and

$$\frac{\partial \tilde{\psi}}{\partial x} = 0 \qquad (y = 0) \qquad (34a)$$

$$\nabla \tilde{\psi} \to 0 \qquad (|x| \to \infty;\ y \to \infty) \qquad (34b)$$

The averages $\langle \varepsilon^{-1} \bar{u} \rangle$ and $\langle \varepsilon^{-1} \bar{v} \rangle$ in equation (31) represent the bulk contributions of the velocity field induced by the moving vortical spots. It can be shown that these averages remain O(1) with respect to ε. (See the appendix.) It then follows that the grid size ΔL and the time step Δt can be selected independent of ε or the core sizes δ_k.

The vorticity deviation $\tilde{\zeta}$ is updated by the finite-difference equation (eq. (31)) using the two-step Lax-Wendroff procedure (ref. 8). The fast Poisson solver (ref. 9) is then used to determine the corresponding stream function $\tilde{\psi}$ from equation (32) for a finite computational domain. The computational domain and the approximate boundary conditions will be described in subsection 3.3. The trajectories of the vortical spots are then defined simultaneously by the integration of equation (28).

Since the average has to be used only when the core size is much smaller than the grid size, the numerical method shall be discussed for the case of $\delta_k << \Delta L$. The integration domain size H is chosen to be of the order of the grid size (e.g., $H = \Delta L/4$). Therefore, H is much less than the normal length scale but is independent of the small core size. Whenever a grid point (x_i, y_j) is far from a vortical spot centered at (X_k, Y_k) (e.g., if $r_k >> H$, then $r_k > CH$), the result is

$$\langle \varepsilon^{-1} \bar{u}_k \rangle = \frac{-\Gamma_k (y_j - Y_k)}{2\pi r_k^2} \left[1 + O\left(\frac{H^4}{r_k^4} \right) \right] \qquad (35a)$$

$$\langle \varepsilon^{-1} \bar{v}_k \rangle = \frac{\Gamma_k (x_i - X_k)}{2\pi r_k^2} \left[1 + O\left(\frac{H^4}{r_k^4} \right) \right] \qquad (35b)$$

where

$$r_k = \left[(x_i - X_k)^2 + (y_j - Y_k)^2 \right]^{1/2}$$

The difference between the average and the classical theory is actually less than 0.6 percent for $C = 2.5$. Therefore, by adjusting C, the transition from the classical solution to the average can be made smaller than the error of the finite-difference method. Only in the region where $r_k \leq CH$ do the averages $\langle \varepsilon^{-1}\bar{u} \rangle$ and $\langle \varepsilon^{-1}\bar{v} \rangle$ need to be evaluated (which are defined by two elementary line integrals, as noted in the appendix).

3.3 Boundary Conditions on a Finite Computational Domain

For the numerical solution of equations (31) to (34) for variations in the background shear flow, one has to work with a finite computational domain D, i.e., $|x| \leq L_1$ and $0 \leq y \leq L_2$. (See fig. 2.) Note that $U_0(y)$ is a solution of the Navier-Stokes equation with a no-slip boundary condition. The boundary layer induced by the disturbed flow shall be ignored; hence, the vortical spot should be "far away" from the ground relative to the core size. Also, the use of the asymptotic solutions (eqs. (25) and (26)) for each core structure requires that the vortical spots be "far apart" from each other. Therefore, the present solution will be applicable only when each vortical spot is several core sizes above the ground and away from the other spots. In order to average over only one vortical spot, the requirement is that the distances from one spot to the ground and to another spot remain greater than twice the grid size, i.e., $2\,\Delta L$.

Note that the boundary condition $\tilde{\psi} = 0$ at $y = 0$ is fulfilled when the image $\tilde{\zeta}(x,-y) = -\tilde{\zeta}(x,y)$ is introduced. The far-field boundary condition (eq. (34b)) has to be replaced by appropriate conditions on the outer boundary of the domain D, i.e., $|x| = L_1$ and $y = L_2$. With $\rho = (x^2 + y^2)^{1/2}$ denoting the distance from the origin, it is seen that when the disturbance velocity behaves as ρ^{-n}, the behaviors of the perturbed stream function $\tilde{\psi}$ and vorticity $\tilde{\zeta}$ are $\tilde{\psi} \approx \rho^{-n+1}$ and $\tilde{\zeta} \approx \rho^{-n-1}$, respectively. Since the flow field induced by the vortical spots is symmetric with respect to the ground ($y = 0$), the variation $\tilde{\zeta}$ of the background vorticity ω_0 has to be antisymmetric with respect to $y = 0$ (with $\tilde{\zeta} = 0$ at $y = 0$) and approaches 0 near the outer boundary. Note that $n = 2$ and 3 for a single spot and for an equal and opposite pair of spots, respectively. Consequently, the boundary condition $\tilde{\zeta} = 0$ can be imposed on the outer boundary ($|x| = L_1$) and on $y = L_2$, with an error smaller than $O(L_i^{-3})$ for a single spot and smaller than $O(L_i^{-4})$ for a vortical pair of spots. On the boundary of D, the condition to be imposed is

$$\tilde{\zeta} = 0 \tag{36}$$

Since the solution $\tilde{\psi}$ can be expressed in terms of a Poisson integral of $\tilde{\zeta}$, the boundary data for $\tilde{\psi}$ can then be evaluated by the far-field expansion of the Poisson integral (ref. 5).

The leading two terms involve only the y- and xy-moments of $\tilde{\zeta}$; i.e., at the boundary where $y = L_2$ or $|x| = L_1$, the expansion is

$$\tilde{\psi} \approx \frac{1}{\pi}\left(\frac{y}{r^2}\int_{-L_1}^{L_1}\int_{0}^{L_2} y'\tilde{\zeta}\, dx'\, dy' + \frac{2xy}{r^4}\int_{-L_1}^{L_1}\int_{0}^{L_2} x'y'\tilde{\zeta}\, dx'\, dy'\right) \tag{37}$$

where $r = \rho = (x^2 + y^2)^{1/2}$. The error of this approximation (eq. (37)) is $O(L_i^{-3})$. Since the error introduced by the finite-difference approximations for equations (31) and (32) are $O((\Delta L)^2)$, ΔL can be related to L_i so that the errors are of the same order in the approximate boundary conditions and in the finite-difference approximations. Using the boundary data from equation (37) and the condition in equation (34a), equation (31) is solved by a fast Poisson solver (ref. 9) to obtain $\tilde{\psi}$ in D, and then the derivatives of $\tilde{\psi}$ yield $\tilde{u}$ and $\tilde{v}$.

4 RESULTS AND DISCUSSION

A computer code based on the previous analysis was developed. Numerical results of the trajectories of vortical spots in a nonuniform shear flow are obtained. For the results reported here, the conditions $L_1 = 8L$, $L_2 = 8L$, and $\Delta x = \Delta y = L/5$ have been chosen. The time step fulfills the condition that the Courant-Friedrichs-Lewy (CFL) number is less than 0.5. The velocity in the CFL number is the maximum of the resultant velocity in equation (31) for all grid points. Test cases were performed for larger L_1 and L_2 and for smaller Δx and CFL number. In all these test cases, the changes in the results are insignificant. To gain a qualitative understanding of the interaction of vortical spots with a background shear flow, the case of a single vortical spot is studied initially. Then, the cases of a vortical pair simulating the trailing vortices are studied.

Figure 3 shows the trajectories of a single concentrated decaying vortical spot of various strengths submerged in a background shear flow. The initial vertical position of the spot is at $y = 1$, and the initial background shear flow is chosen as $U_0(y) = 1 - e^{-y}$. The results show that the vortical spots with positive circulation drift spanwise (x-direction) and upward (y-direction), and the vortical spots with negative circulation drift spanwise and downward but eventually turn backward. This phenomenon is more pronounced as the strength of the vortical spot increases.

To explain this phenomenon, the case of a single vortical spot with $\Gamma > 0$ is considered. The disturbed flow moves downward behind the spot ($x < X$) and upward ahead of the spot ($x > X$). For an initial background vorticity ω_0 with $\omega_0'(y) > 0$ (see eqs. (2) and (3)), the disturbed flow increases the vorticity behind the spot and decreases the vorticity ahead of it; i.e., $\tilde{\zeta} > 0$ for $x < X$ and $\tilde{\zeta} < 0$ for $x > X$. The background vorticity variation $\tilde{\zeta}$ in turn induces an upward motion of the vortical spot for $\Gamma > 0$. From similar arguments, it can be expected that the background vorticity variation $\tilde{\zeta}$ will induce a downward motion of the vortical spot with $\Gamma < 0$. The reason that a vortical spot of negative strength turns around and drifts upstream as it gets closer to the ground can be attributed to the decrease of the contribution of the background shear flow to the forward velocity of the spot and to the increase of the induced velocity by the image of the vortical spot with respect to the ground ($y = 0$). It should be pointed out here once more that the vortical spot will drift horizontally when the background shear flow is either a uniform flow ($\omega_0 = 0$) or a constant shear flow ($\omega_0 = \text{Constant}$), and there will be no change in the background flow ($\tilde{\zeta} = 0$).

The trailing-vortex wakes far downstream of an aircraft shall be simulated by a simple vortex pair whose vorticity distributions are concentrated and are centered at $(\pm X_k(0), Y_k(0))$ with strength $\pm\Gamma$ and effective vortical size $\delta(0)$. The goal of the following numerical examples is to simulate the interaction of the decaying trailing vortical pairs subjected to a crosswind (spanwise) ground shear. The background shear flow used in the examples is again an exponential profile (eq. (2b)) unless otherwise specified.

Figure 4 shows the relative trajectories, i.e., the variation of the vertical positions versus the horizontal spread of a vortex pair whose strengths are $\Gamma = \pm 1$. Solid curves show the relative trajectories of a vortex pair descending without a background shear flow. Dashed-line curves show the corresponding trajectories of vortex pairs with an initial location at $(\pm 0.5, 3)$ and $(\pm 0.5, 4)$ under the influence of ground shear wind. The vertical position of the left vortex shows that it drifts to the left and continuously descends in time, whereas the right vortex descends initially until it reaches a minimum height and then drifts upward. Because $x = 0$ has been set at the mean position of the vortical pair, this curve does not show the real spanwise position and does not see the eventual backward drift of the left vortical spot. This backward drift occurs when the background vorticity variation finally overcomes the downward velocity induced on the right vortex center by the left vortex. This effect is in contrast to the case when the background flow is uniform or of constant shear flow, for which the vortex spots will keep on drifting apart and downward.

In order to find out when the shear-layer solution has to be used, the trajectories of a pair of vortices in a shear layer for different initial vortex heights are studied. The minimum height reached by the right vortical spot $Y_{R,min}$ is plotted against the initial height of the vortical pair in figure 5. The height $Y_{R,min}$ approaches an asymptotic value of 2.6 when $Y_k(0)$ is greater than 7.0. This event means that when the vortical spots are above $y = 7$, they are far above the shear layer and the interaction with the shear layer is negligible. The corresponding trajectories (in real spanwise positions) of the vortical pair, starting at different heights $Y_k(0) = 1, 2, 3, 4,$ and 5 in the shear layer, are displayed in figure 6 to show that the trajectories of the vortical spots are sensitive to the starting height (i.e., the altitude of the airplane relative to the thickness of the shear layer).

The initial strength of the vortical spots also has a significant effect on the trajectories of decaying trailing vortices in a ground shear, as illustrated in figure 7. The initial positions of the vortical spots are $(X_k(0), Y_k(0)) = (\pm 0.5, 3.0)$. The vortical pairs of stronger strength $(\Gamma = \pm 4)$ descend faster and drift less in horizontal (spanwise) distance as compared with the vortical pair of strength $\Gamma = \pm 1$, since the initial downward drift is dominated by their strength Γ. The vortical spot on the right side, with vorticity in an opposite sense to that of the shear flow, descends to a lower minimum elevation for larger Γ.

Finally, the interaction effects of different background flows are studied. A comparison is made for a background exponential profile with a Blasius profile of the same thickness; i.e., the length of the profile is equal to L^2U_∞/ν. The initial positions of the vortex pair are $(X_k(0), Y_k(0)) = (\pm 0.5, 4.0)$ and their strengths are $\Gamma = \pm 1$. Figure 8 demonstrates that the effect of the crosswind shear profile on the behavior of trajectories for the left vortex is small but the right vortex descends much less; i.e., it descends to a larger $Y_{R,min}$ for the Blasius profile as compared with the exponential profile.

5 CONCLUDING REMARKS

A computer code has been developed for the study of rotational flow fields having concentrations of large-magnitude vorticity in spots (small areas). The analysis takes into account the small scale of the flow field near a spot and the normal scale for the background flow. Using this two-length-scale analysis, the decay of the vortical spots (in small scale) is obtained analytically and the motion of the spot is coupled with transport of the background vorticity, which is analyzed by numerical solution of the Euler equation. The particular feature of the numerical method is that the grid size for the numerical analysis can be chosen independent of the size of the vortical core, and hence the time step is also independent of the core size.

Numerical examples for a single vortical spot submerged in a background shear flow shows that the variation of the background shear flow induces an upward motion for the vortical spot with positive circulation and induces a downward motion for the vortical spot with negative circulation. The latter eventually reverses its direction of horizontal drift when it gets close to the ground where the ground effect overcomes the smaller forward shear flow velocity. This interaction between the vortical spots and the background flow is absent if the background flow is of constant vorticity or is a uniform flow, for which the vortical spot will only drift horizontally.

For a pair of vortical spots simulating trailing vortices in a crosswind, the result shows that both vortices will initially drift forward together, spread apart, and move downward. Gradually, under the effects of interaction, the redistribution of the background vorticity changes the trajectories. The vortex that is in the opposite sense to that of the background flow will reach a minimum height, reverse its downward drift, and turn upward, whereas the other vortex will eventually reverse its forward motion and turn backward. When the vortical pair is submerged in different background flows, namely the Blasius and exponential profiles, the numerical examples show that the trajectories of the vortical pair are similar in nature but quantitatively different.

NASA Langley Research Center
Hampton, Virginia 23665-5225
May 22, 1986

APPENDIX

AVERAGE OF THE VELOCITY INDUCED BY kth VORTICAL SPOT $\langle \varepsilon^{-1}(\bar{u}_k \hat{i} + \bar{v}_k \hat{j}) \rangle$

It is necessary to derive the formula for the average velocity at a grid point (x_i, y_j) that is close to the kth spot centered at (X_k, Y_k), with $|x_i - X_k| < H$ and $|y_j - Y_k| < H$. (See fig. A1.)

Because of the symmetry of the velocity field with respect to the vortical center (X, Y), the formula for $\langle \varepsilon^{-1}\bar{u} \rangle$ shall be derived. The formula for $\langle \varepsilon^{-1}\bar{v} \rangle$ is equal to that for $\langle \varepsilon^{-1}\bar{u} \rangle$ with x_i and X interchanged with y_j and Y, respectively. The restriction to be imposed is that

$$H > X - x_i \geq 0 \qquad H > Y - y_j \geq 0 \tag{A1}$$

Since $\bar{u}$ is asymmetric with respect to $y = Y$, the result is

$$\langle \varepsilon^{-1}\bar{u} \rangle = \frac{-\Gamma}{8\pi H^2} \int_{-H}^{H} dx' \int_{-H}^{2(Y-y_j)-H} dy' \frac{y_j + y' - Y}{(r')^2} \left[1 - e^{-(r'/\delta)^2}\right]$$

where

$$r' = [(x_i + x' - X)^2 + (y_j + y' - Y)^2]^{1/2}$$

The integration can be carried out with respect to y' and then a definite integral is obtained, i.e.,

$$\langle \varepsilon^{-1}\bar{u} \rangle = -\frac{\Gamma}{16\pi H^2} \int_{-H}^{H} dx' \int_{R^-}^{R^+} \frac{dR}{R}(1 - e^{-R}) \tag{A2}$$

$$\langle \varepsilon^{-1}\bar{u} \rangle = -\frac{\Gamma}{16\pi H^2} \int_{-H}^{H} dx' \left[\ln R + E_1(R)\right]_{R^-}^{R^+} \tag{A3}$$

where

$$R^{\pm} = \left[(x_i - X)^2 + (Y - y_j \pm H)^2\right]/\delta^2$$

and $E_1(R)$ is the exponential integral of R (ref. 10).

From equation (A2) it can be shown that the integral with respect to R is finite; hence, $\langle \varepsilon^{-1}\bar{u} \rangle$ is $O(1)$ with respect to ε. This result is also true for $\langle \varepsilon^{-1}\bar{v} \rangle$.

Note that when R is greater than 2, $E_1(R)$ is negligible and the integral in equation (A3) can be evaluated explicitly. Therefore, numerical evaluation of the integral in equation (A3) is needed only for $r' \leq 2\delta$.

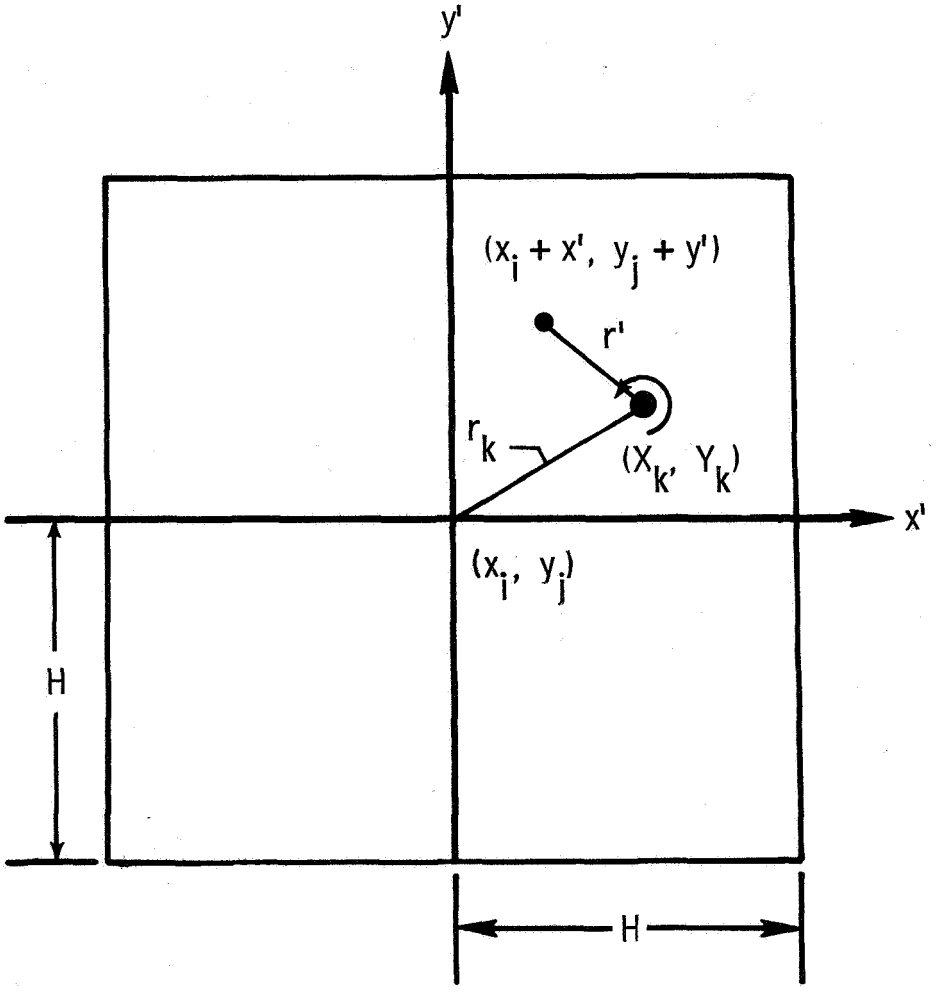

Figure A1.- "Average" square domain.

REFERENCES

1. Olsen, John H.; Goldburg, Arnold; and Rogers, Milton, eds.: Aircraft Wake Turbulence and Its Detection. Plenum Press, 1971.

2. Wake Vortex Minimization. NASA SP-409, 1977.

3. Steger, Joseph L.; and Kutler, Paul: Implicit Finite-Difference Procedures for the Computation of Vortex Wakes. AIAA J., vol. 15, no. 4, Apr. 1977, pp. 581-590.

4. Ting, L.: Studies on the Motion and Decay of a Vortex Filament. Advances in Fluid Mechanics, Volume 148 of Lecture Notes in Physics, E. Krause, ed., Springer-Verlag Berlin Heidelberg New York, 1981, pp. 67-105.

5. Lamb, Horace: Hydrodynamics, Sixth ed. Dover Publ., Inc., 1945.

6. Ting, L.; and Tung, C.: Motion and Decay of a Vortex in a Nonuniform Stream. Phys. Fluids, vol. 8, no. 6, June 1965, pp. 1039-1051.

7. Ting, Lu: On the Application of the Integral Invariants and Decay Laws of Vorticity Distributions. J. Fluid Mech., vol. 127, Feb. 1983, pp. 497-506.

8. Richtmyer, Robert D.; and Morton, K. W.: Difference Methods for Initial-Value Problems, Second ed. Interscience Publ., c.1967.

9. Swarztrauber, Paul N.; and Sweet, Roland A.: ALGORITHM 541, Efficient FORTRAN Subprograms for the Solution of Separable Elliptic Partial Differential Equations [D3]. ACM Trans. Math. Software, vol. 5, no. 3, Sept. 1979, pp. 352-364.

10. Abramowitz, Milton; and Stegun, Irene A., eds.: Handbook of Mathematical Functions With Formulas, Graphs, and Mathematical Tables. NBS Appl. Math. Ser. 55, U.S. Dep. Commerce, June 1964.

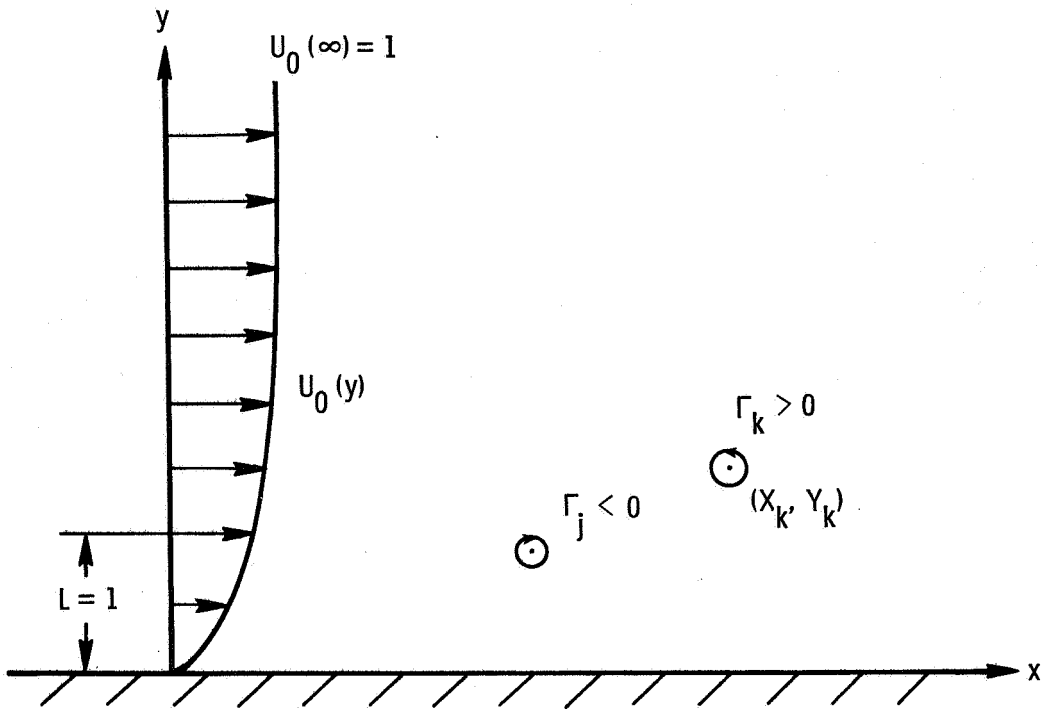

Figure 1.- Physical model for motion and decay of vortical spots submerged in ground wind shear.

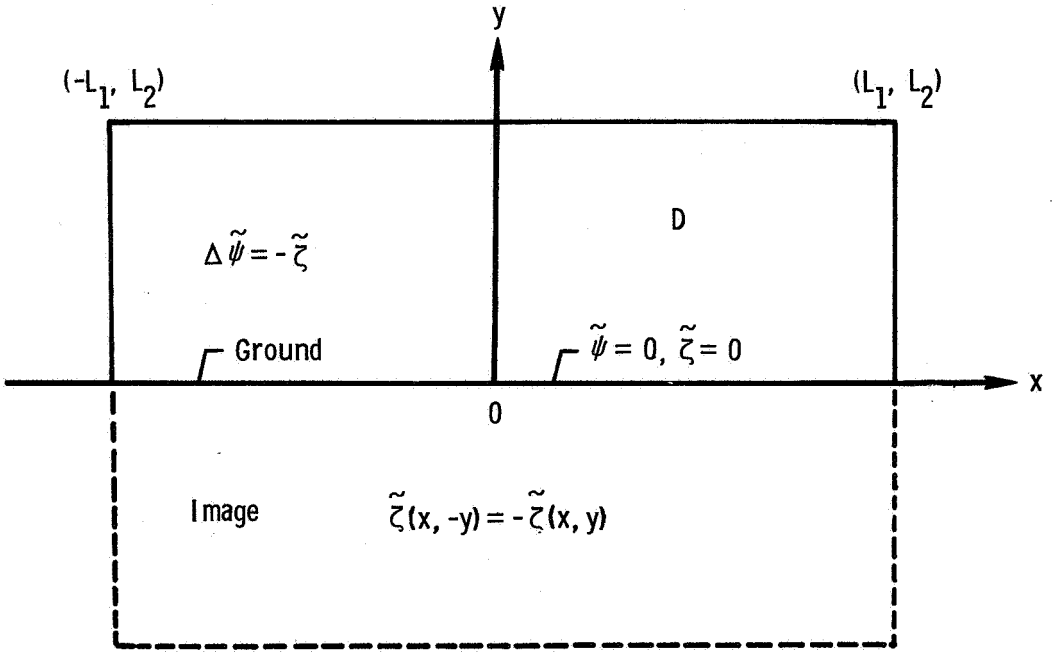

Figure 2.- Finite computational domain and boundary conditions.

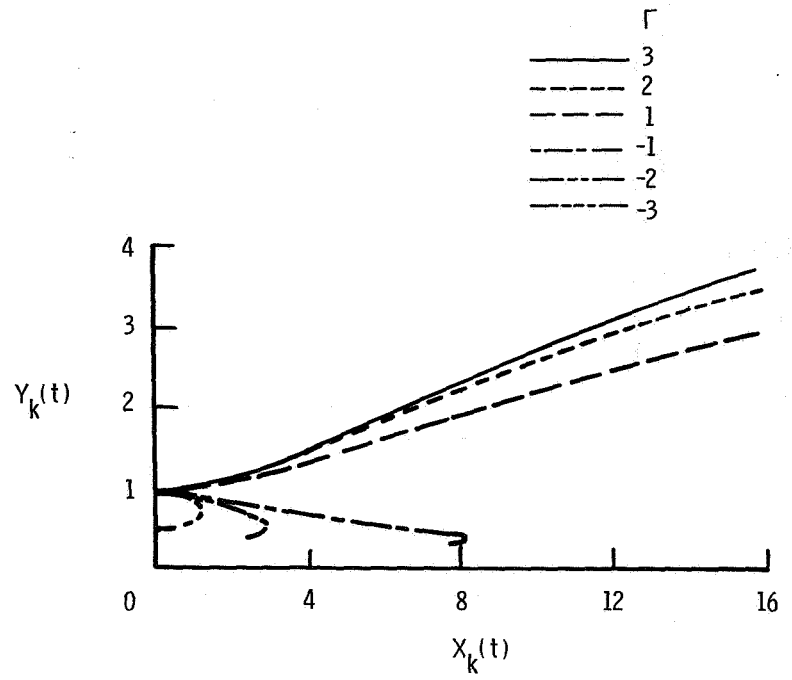

Figure 3.- Effect of strength on trajectory of single vortical spot in shear flow.

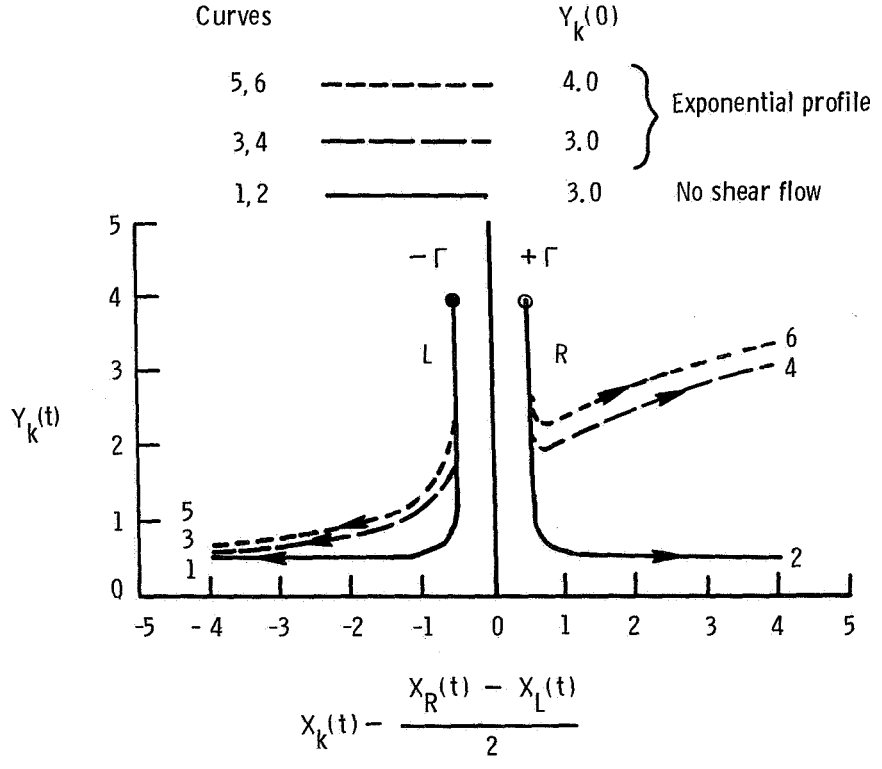

Figure 4.- Comparison of trajectory of vortical pair in shear flow with uniform flow. Left and right are denoted by L and R, respectively.

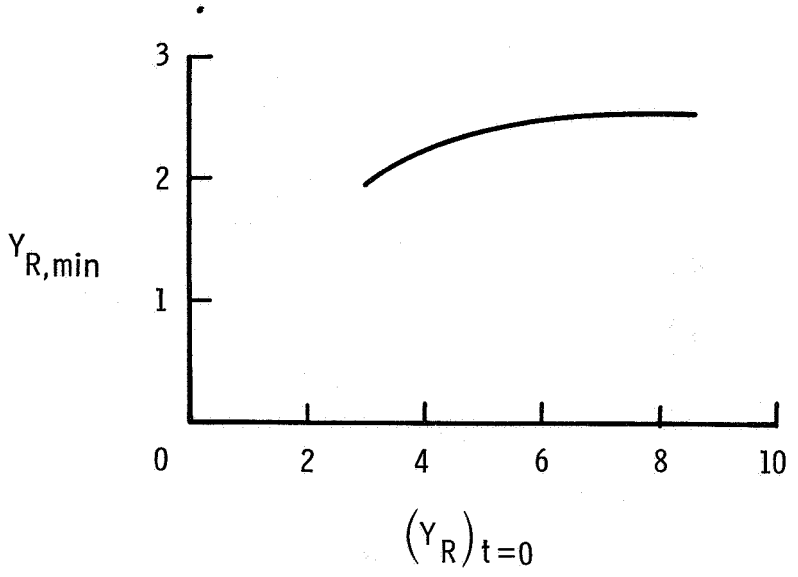

Figure 5.- Minimum vertical position as function of initial height for vortical spot on right side.

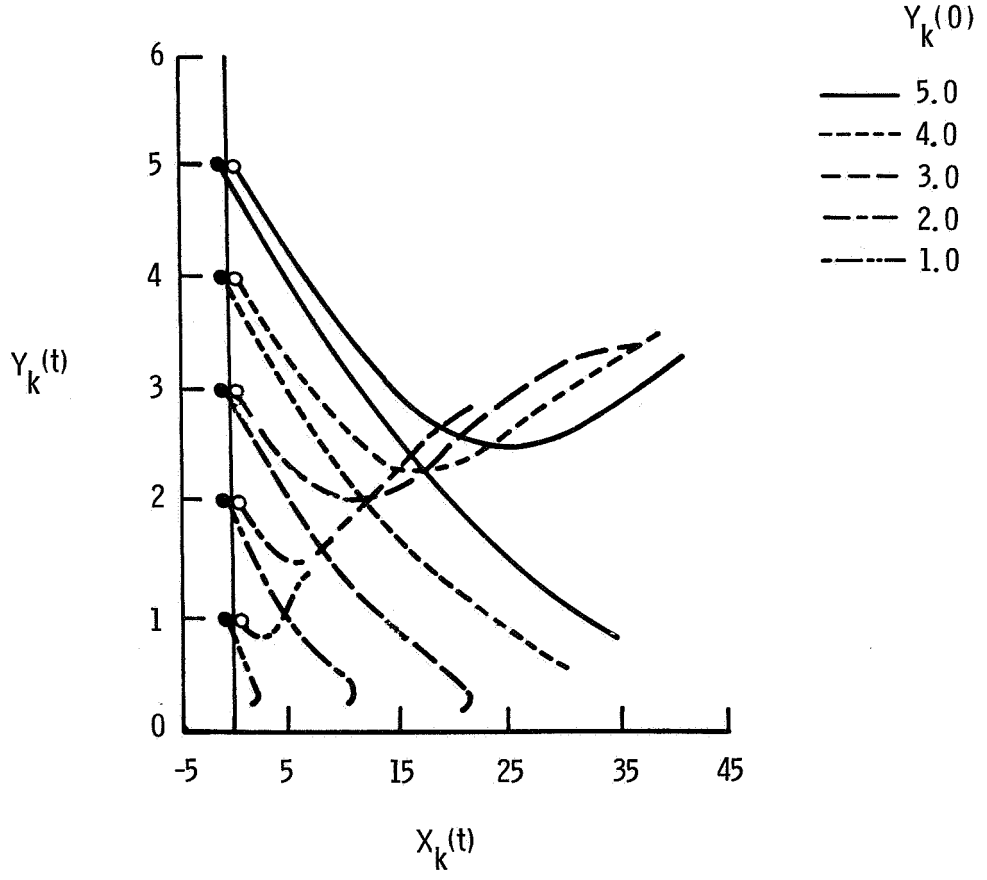

Figure 6.- Comparison of trajectories of vortical pair cutting shear flow with different initial positions.

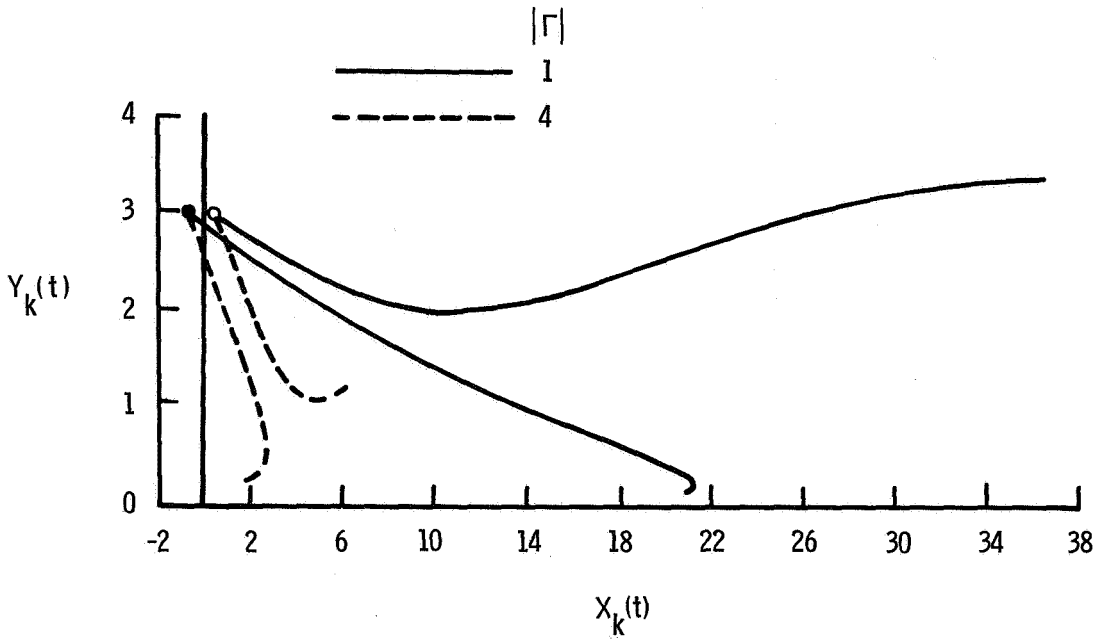

Figure 7.- Effect of vortical-pair strength on trajectories.

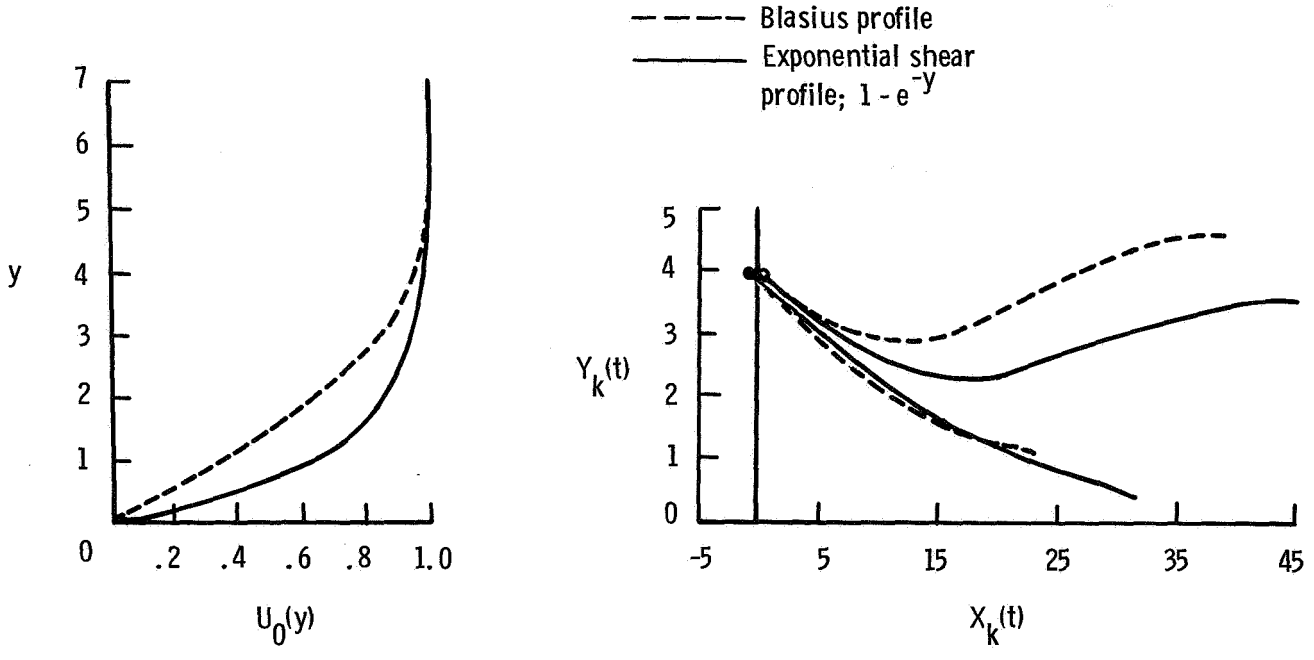

Figure 8.- Trajectories of vortical pair for different background shear flows.

Standard Bibliographic Page

1. Report No.	2. Government Accession No.	3. Recipient's Catalog No.
NASA TP-2599		

4. Title and Subtitle	5. Report Date
Motion and Interaction of Decaying Trailing Vortices in Spanwise Shear Wind	September 1986
	6. Performing Organization Code: 505-60-21-03
7. Author(s): Chen-Huei Liu and Lu Ting	8. Performing Organization Report No.: L-16040
9. Performing Organization Name and Address: NASA Langley Research Center, Hampton, VA 23665-5225	10. Work Unit No.
	11. Contract or Grant No.
12. Sponsoring Agency Name and Address: National Aeronautics and Space Administration, Washington, DC 20546-0001	13. Type of Report and Period Covered: Technical Paper
	14. Sponsoring Agency Code

15. Supplementary Notes

Chen-Huei Liu: Langley Research Center, Hampton, Virginia.
Lu Ting: New York University, New York, New York.

16. Abstract

This paper presents a simulation of the drift of trailing vortices in a cross-wind near the ground by an unsteady, two-dimensional, rotational flow field with a concentration of large vorticity in "vortical spots" (having a finite but small effective size and finite total strength). The problem is analyzed by a combination of the method of matched asymptotic analyses for the decay of the vortical spots and the Euler solution for the unsteady rotational flow. Using the method of averaging, a special numerical method is developed in which the grid size and time step depend only on the length and velocity scales of the background flow and are independent of the effective core size of a vortical spot. The core size can be much smaller than the grid size, whereas the peak velocity in the core is inversely proportional to the spot size. Numerical results are presented to demonstrate the strong interaction between the trajectories of the vortical spots and the change of the vorticity distribution in the background flow field.

17. Key Words (Suggested by Authors(s))	18. Distribution Statement
Vortical flows Vortex/shear-flow interaction Trailing vortex wakes	Unclassified - Unlimited Subject Category 01

19. Security Classif.(of this report)	20. Security Classif.(of this page)	21. No. of Pages	22. Price
Unclassified	Unclassified	22	A02

For sale by the National Technical Information Service, Springfield, Virginia 22161

NASA-Langley, 1986